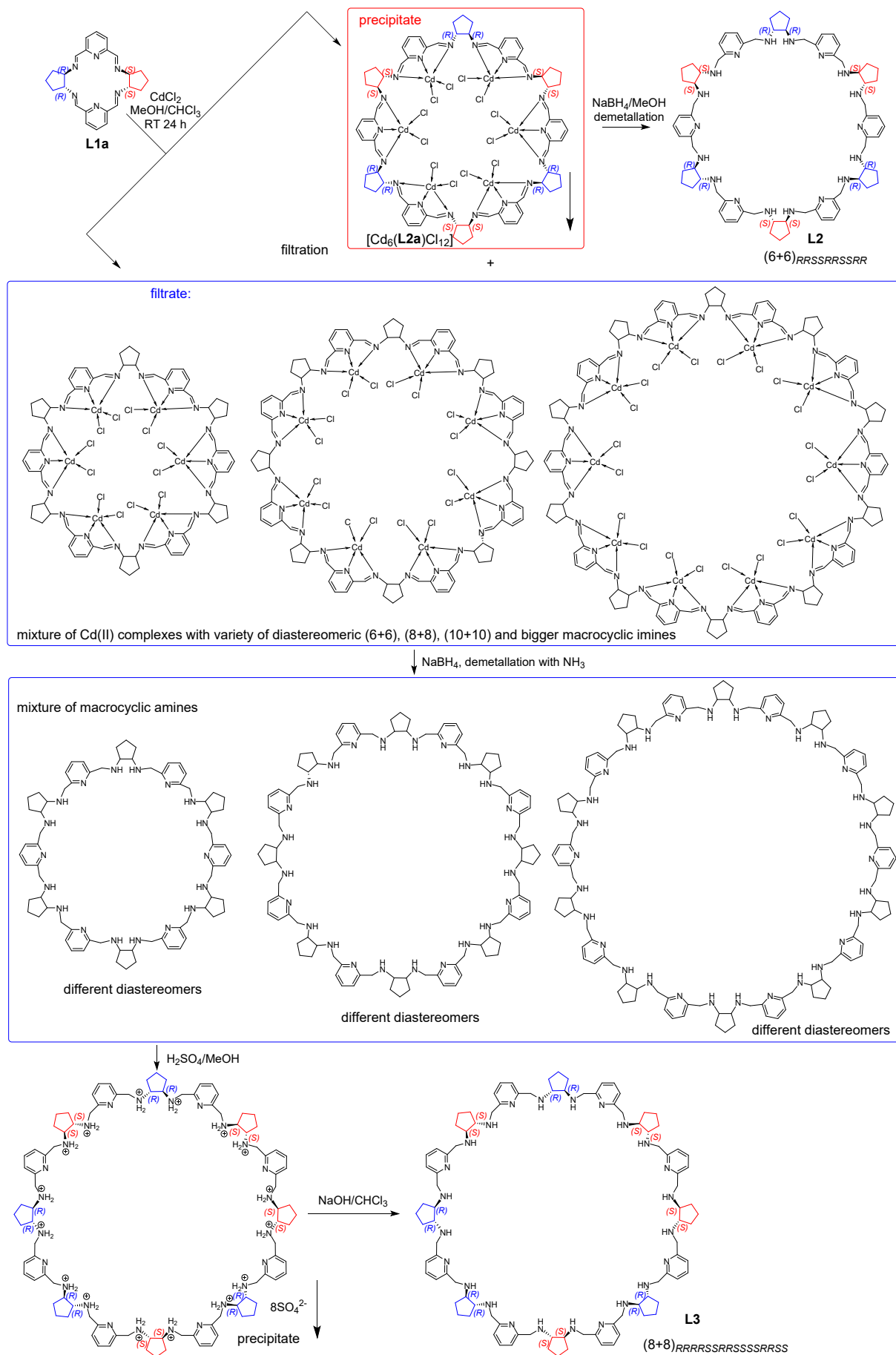Supporting Information

Hexa- and octanuclear copper(II) complexes with tetraeicosaaza amine macrocycle
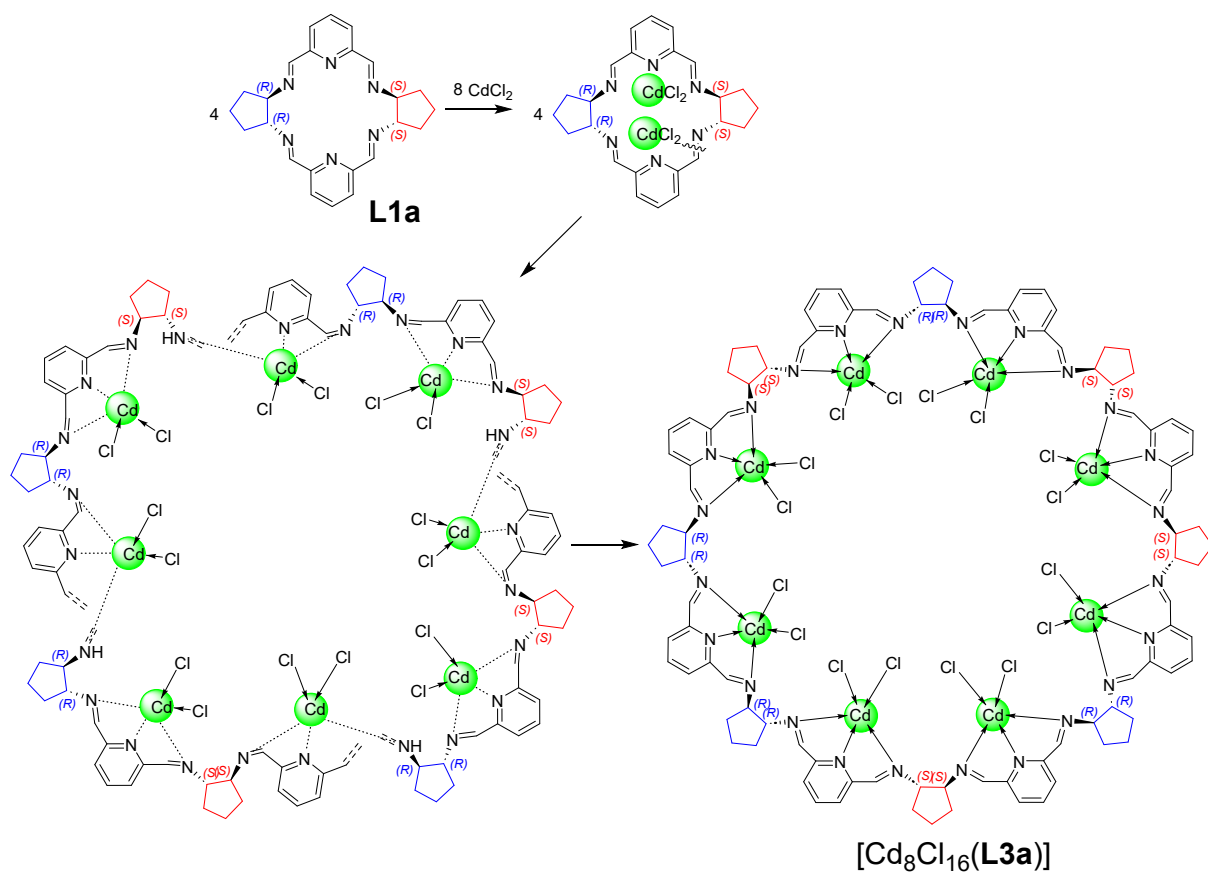
Dominika Fedorowicz[a], Katarzyna Ślepokura[a], Julia Kłak[a], Maciaj Witwicki[a] and Janusz Gregoliński[a*]

Content:

Scheme S1. Cd(II) templated synthesis of (6+6) and (8+8) amine macrocycles, **L2** and **L3**, respectively.[19]

Scheme S2. Suggested mechanism of Cd(II) templated formation of (8+8) macrocyclic imine Cd(II) complex, [Cd$_8$Cl$_{16}$(**L3a**)], from (2+2) *meso* imine **L1a**.

Synthesis of macrocyclic ligand

Macrocycle **L3**, $C_{96}H_{136}N_{24}\cdot0.75H_2O$, has been obtained in a large scale in an optimized procedure slightly modified than previously described.[19]

Crude mixture of large amine macrocycles - Cd(II)-templated synthesis

11.40 g (62.18 mmol) of anhydrous $CdCl_2$ were added to the suspension of 4.130 g (10.36 mmol) of (2+2) imine **L1a** in 5500 mL of a methanol/chloroform mixture 1:1 v/v, and the mixture was stirred at room temperature for 24 h. The crude precipitate of the cadmium(II) complex of (6 + 6) imine $[Co_6(\textbf{L2a})Cl_{12}]$ was filtered off (3.95 g, this substance is a substrate for preparation of (6+6) amine **L2**),[3,18] and an excess of $NaBH_4$ (14.40 g) was added in portions with stirring to the filtrate. After 20 h of stirring at room temperature the mixture was evaporated to dryness to give a reddish solid. This dry residue was redissolved in a mixture of 200 mL of 25% ammonia and 200 mL of water and stirred for 30 minutes. Then 200 mL of chloroform was added, and the mixture was vigorously stirred for 3 h. The layers were separated, and the water phase was stirred again twice with 200 mL of fresh chloroform. Organic solutions were combined and dried over anhydrous sodium sulphate.

* - 1 mL of that solution was taken, evaporated to dryness and ^{1}H NMR spectrum of that crude sample was measured to check if the signals are sharp. If yes, the bulk chloroform solution was evaporated do dryness. If not (the broaden signals meant that traces of Cd(II) ions are present in a sample), the procedure of demetallation with new portion of 200 mL of 25% ammonia was repeated, layers were separated , dried over anhydrous sodium sulphate and evaporated to dryness.

Yield 3.59 g of sticky oil of a crude mixture containing the (6+6), (8+8), (10+10) and bigger macrocyclic amines.

Sulfuric acid salt of L3 amine – L3·8H$_2$SO$_4$·32H$_2$O, $C_{96}H_{136}N_{24}\cdot8H_2SO_4\cdot32H_2O$**.**

3.59 g of above mixture of macrocyclic amines was dissolved in 140 mL of methanol and to that solution 5.21 g of 50% sulfuric acid was added in portions. The formed gummy solid was dissolved completely by ultrasonic bath (ca. 30 minutes) to give transparent solution, which after 10 minutes began to go cloudy. After 48 hours the white crystalline precipitate was filtered off and dried in vacuum to give 417.5 mg of pure sulfuric acid salt **L3·8H$_2$SO$_4$·32H$_2$O**. Additional portion of the same substance (147.5 mg) was collected after leaving the flask open for the next 24 hours to concentrate a bit the methanol solution. The combined yield 7.3%.

Free L amine – L3·0.75H$_2$O, $C_{96}H_{136}N_{24}\cdot0.75H_2O$.

200.0 mg (6.735×10^{-5} mol) of the protonated form $C_{96}H_{136}N_{24}\cdot8H_2SO_4\cdot32H_2O$ were treated with 10 mL (20 mmol) of 2 M NaOH solution and extracted three times with 10 mL of chloroform. The combined organic phase was dried over anhydrous sodium sulphate and evaporated to dryness to give 110.4 mg (100%) of free (8 + 8) amine **L3·0.75H$_2$O**.

Synthesis of Cu(II) complexes:

[Cu$_6$(NO$_3$)$_{12}$(**L3**)]·9H$_2$O (**1**).

55.3 mg (3.37·10^{-5} mol) of ligand **L3·0.75H$_2$O** was dissolved in 10 mL of methanol. To that solution 65.1 mg (2.69·10^{-4} mol) of Cu(NO$_3$)$_2$·3H$_2$O was added and the solution was refluxed for 4 hours. The dark blue precipitate was collected by filtration (48.0 mg). The filtrate was concentrated twice and after 4 days the new precipitate was filtered off (15.5 mg). Precipitates were dried in vacuum. The combined yield 63.5 mg (65%). Anal. Calc. (found) for [Cu$_6$(NO$_3$)$_{12}$(C$_{96}$H$_{136}$N$_{24}$)]·9H$_2$O: C, 39.57 (39.59); H, 5.33 (5.40); N, 17.31 (17.33). ESI MS: m/z: 1313.3 for [Cu$_6$L(NO$_3$)$_{10}$]$^{2+}$, 1219.8 for [Cu$_5$L(NO$_3$)$_8$]$^{2+}$, 854.8 for [Cu$_6$**L3**(NO$_3$)$_9$]$^{3+}$, 792.6 for [Cu$_5$**L3**(NO$_3$)$_7$]$^{3+}$, 625.6 for [Cu$_6$**L3**(NO$_3$)$_8$]$^{4+}$ and 578.9 for [Cu$_5$**L3**(NO$_3$)$_6$]$^{4+}$.

Monocrystals **1'** were grown by slow evaporation of methanol/acetonitrile solution of [Cu$_6$(NO$_3$)$_{12}$(**L3**)]·9H$_2$O complex.

[Cu$_8$Cl$_{16}$(**L3**)]·5H$_2$O (**2**).

82.8 mg (5.05·10^{-5} mol) of ligand **L3·0.75H$_2$O** was dissolved in 10 mL of methanol. To that solution 68.9 mg (4.04·10^{-4} mol) of CuCl$_2$·2H$_2$O was added and the solution was refluxed for 4 hours. The mixture was left for 4 days at RT and the blue/green precipitate was collected by filtration (68.4 mg). The filtrate was concentrated twice and after 1 day the new precipitate was filtered off (30.4 mg). Precipitates were dried in vacuum. The combined yield 98.8 mg (70.0%). Anal. Calc. (found) for [Cu$_8$Cl$_{16}$(C$_{96}$H$_{136}$N$_{24}$)]·5H$_2$O: C, 41.30 (41.25); H, 5.27 (5.05); N, 12.04 (11.80). ESI MS: m/z: 1315.0 for [Cu$_8$**L3**Cl$_{14}$]$^{2+}$, 965.1 for [Cu$_8$**L3**Cl$_{13}$]$^{3+}$ and 640.1 for [Cu$_8$**L3**Cl$_{12}$]$^{4+}$.

Monocrystals **2'** were grown by slow diffusion of acetonitrile into a methanol solution of [Cu$_8$Cl$_{16}$(**L3**)]·5H$_2$O complex.

[Cu$_8$(SO$_4$)$_8$(**L3**)·37H$_2$O (**3**).

82.8 mg (5.05·10^{-5} mol) of ligand **L3·0.75H$_2$O** was dissolved in 10 mL of methanol. To that solution 100.9 mg (4.041·10^{-4} mol) of CuSO$_4$·5H$_2$O was added and the solution was refluxed for 4 hours. The mixture was left for 4 days at RT and small amount of blue precipitate was filtered off and discarded. To the filtrate 10 mL of acetonitrile was added and the solution was concentrated on a rotary evaporator till blue precipitate appeared. The flask was kept in freezer for several days and the blue precipitate was collected by filtration, washed with 1 mL of cold acetonitrile and dried in vacuum. The obtained precipitate was dried in vacuum. The yield 136.9 mg (75.6%). Anal. Calc. (found) [Cu$_8$(SO$_4$)$_8$(C$_{96}$H$_{136}$N$_{24}$)]·37H$_2$O: C, 32.30 (32.23); H, 5.93 (5.57); N, 9.42 (9.26). ESI MS: m/z: 1403.1 for [Cu$_8$**L3**(SO$_4$)$_{10}$]$^{2+}$ and 935.7 for [Cu$_8$**L3**(SO$_4$)$_6$(HSO$_4$)]$^{3+}$.

Monocrystals **3'** by slow diffusion of acetonitrile into a water solution of [Cu$_8$(SO$_4$)$_8$(**L3**)·37H$_2$O complex.

X-ray crystallography

X-ray diffraction data for the crystals were collected at 100 K on a κ-geometry Rigaku XtaLAB Synergy DW diffractometer with Cu$K\alpha$ radiation (ω scans, rotating-anode X-ray source). Data collections, cell refinements, data reductions and analyses, including empirical (multi-scan) absorption corrections, were carried out with *CrysAlisPRO*.[39] With the use of Olex2,[40] structures were solved with *SHELXT* program[41] employing dual-space algorithm, and refined on F^2 by a full-matrix least-squares procedure using *SHELXL* program[42] with anisotropic displacement parameters for the fully occupied non-H atoms. Some positions of partially occupied atoms were also refined anisotropically.

H atoms in all the crystal structures were found in the difference Fourier maps or were included using geometrical considerations. In the final refinement cycles, all C-bound and most of the N-bound H atoms were repositioned in their calculated positions and were refined using a riding model, with N–H = 1.0 Å and C–H = 0.95-1.00 Å, and with U_{iso}(H) = 1.2U_{eq}(N,C) for NH, CH, CH$_2$ or 1.5U_{eq}(C) for CH$_3$. H atoms from one of the ligand NH groups and bridging OH in **1'** were refined with N–H and O–H distances restrained to 1.000(2) and 0.840(2), respectively. Water H atoms were refined with O–H and H···H distances restrained to 0.840(2) and 1.360(2) Å, respectively, and with U_{iso}(H) = 1.5U_{eq}(O). In the final cycles, for water H atoms a rigid-body model was used or they were constrained to ride on their parent atoms (AFIX 6, AFIX 7 or AFIX 3 instructions). H atoms of some water molecules in **1'**, **2'** and **3'** (SOF < 1) were not found in difference Fourier maps, as stated below.

Disorder of the ligands, NO$_3^-$, Cl$^-$ and SO$_4^{2-}$ anions and solvent molecules. All the crystals are centrosymmetric (triclinic space group $P\bar{1}$) and Z' = 0.5. Ligands in all crystals were found to be partially disordered. In **1'**, the –NH–CH$_2$–Py–CH$_2$– fragment (Py = pyridine) was modelled in three positions with SOFs = 0.456(5), 0.317(5) and 0.229(5), which were restrained to sum up to 1.000(1) with the use of SUMP instruction. Two higher-occupied positions were refined anisotropically. In **2'**, a small fragment of cyclopentane ring (CP) was refined anisotropically in two positions with SOFs = 0.54(2) and 0.46(2). An interestingly disordered ligand was observed in **3'**. Here, the refinement of the –NH–CH$_2$–Py–CH$_2$–NH–CP–HN– fragment in two positions, with SOFs = 0.723(8) and 0.277(8), revealed opposite absolute configuration of DACP fragments. As a consequence, two different coordination modes of the same ligand may be considered, as shown in Figure S1.

All nitrate anions in **1'** were refined (mainly anisotropically, see details in the CIF file) in two or three positions each. Only one from uncoordinated water molecules is fully occupied (site occupation factor, SOF = 1.0). Remaining are highly disordered into nine positions, which were refined isotropically with SOF = 0.25 or 0.5. Their H atoms were not found in difference Fourier maps.

Only one from uncoordinated chloride anions in **2'** is fully occupied. Remaining five positions were refined anisotropically with SOF constrained to 0.75 or 0.5. Acetonitrile molecule was refined anisotropically with SOF = 0.5. Seven of the twelve water positions were found to be partially occupied and were refined without H atoms, with SOFs = 0.25, 0.5, 0.57(2) and 0.43(2). Oxygen atom positions with SOF > 0.25 were refined anisotropically.

Two from three uncoordinated sulfate anions in **3'** were found to be disordered into three or two positions each. Positions with SOF > 0.4 were refined anisotropically. There are 28 positions of water molecules, nine of which are fully occupied. Remaining were refined (mainly isotropically, see details in the CIF file) with SOF from 0.2 to 0.75. With the exception of two positions, their H atoms were not found in difference Fourier maps.

Due to disorder in the solvent regions of the crystals, their formulae, i.e. $[Cu_6L(OH)_2(H_2O)_2](NO_3)_{10}\cdot7.5H_2O$ for **1'**, $[Cu_8LCl_8]Cl_8\cdot CH_3CN\cdot16H_2O$ for **2'** and $[Cu_8L(SO_4)_2(H_2O)_{16}](SO_4)_6\cdot2CH_3CN\cdot33.5H_2O$ for **3'**, should be treated as an approximation.

Figures presenting the molecular structures were made using the Mercury[43] or DIAMOND[44] program. Details of structures refinements are given in Table S1 and the crystallographic information files (CIFs) deposited at the Cambridge Crystallographic Data Centre (CCDC Nos. 2290069-2290071) and provided as Supplementary Data.

Table S1. Crystal data for **1'**, **2'** and **3'**.

	$[Cu_6L3(OH)_2(H_2O)_2](NO_3)_{10}$ $\cdot7.5H_2O$, **1'**	$[Cu_8L3Cl_8]Cl_8\cdot CH_3CN$ $\cdot16H_2O$, **2'**	$[Cu_8L3(SO_4)_2(H_2O)_{16}](SO_4)_6$ $\cdot2CH_3CN\cdot33.5H_2O$, **3'**
CCDC No.	2290069	2290070	2290071
Chemical formula	$C_{96}H_{157}Cu_6N_{34}O_{41.5}$	$C_{98}H_{171}Cl_{16}Cu_8N_{25}O_{16}$	$C_{100}H_{241}Cu_8N_{26}O_{81.5}S_8$
M_r	2832.79	3031.11	3876.97
Crystal system, space group	Triclinic, $P\overline{1}$	Triclinic, $P\overline{1}$	Triclinic, $P\overline{1}$
Temperature (K)	100(2)	100(2)	100(2)
a, b, c (Å)	14.445(3), 14.703(3), 15.916(3)	10.065(2), 18.867(5), 19.228(4)	15.591(3), 17.137(2), 18.252(3)
α, β, γ (°)	108.45(2), 93.03(2), 103.86(2)	109.78(2), 95.56(2), 97.30(2)	104.80(2), 104.09(2), 112.11(2)
V (Å^3)	3082.7(12)	3369.5(14)	4042.0(13)
Z	1	1	1
Radiation type	Cu $K\alpha$	Cu $K\alpha$	Cu $K\alpha$
μ (mm^{-1})	1.95	4.80	3.02
Crystal size (mm)	0.21 × 0.02 × 0.02	0.06 × 0.03 × 0.02	0.10 × 0.05 × 0.03
Diffractometer	Rigaku XtaLAB Synergy R, DW system with HyPix-Arc 150 detector	Rigaku XtaLAB Synergy R, DW system with HyPix-Arc 150 detector	Rigaku XtaLAB Synergy R, DW system with HyPix-Arc 150 detector
Absorption correction	Multi-scan	Multi-scan	Multi-scan
T_{min}, T_{max}	0.092, 1.000	0.814, 1.000	0.743, 1.000
No. of measured, independent and observed [$I > 2\sigma(I)$] reflections	124554, 12402, 11308	37183, 11541, 8463	55035, 15514, 10376
R_{int}	0.046	0.078	0.049
$(\sin \vartheta/\lambda)_{max}$ (Å^{-1})	0.629	0.595	0.622
$R[F^2 > 2\sigma(F^2)]$, $wR(F^2)$, S	0.058, 0.172, 1.05	0.082, 0.251, 1.04	0.069, 0.213, 1.06
No. of reflections	12402	11541	15514
No. of parameters	1127	804	1133
No. of restraints	463	24	421
$\Delta\rho_{max}$, $\Delta\rho_{min}$ (e Å^{-3})	0.77, −0.58	1.31, −1.02	0.68, −0.90

Computer programs: *CrysAlis PRO* 1.171.41.80a (Rigaku OD, 2020), *CrysAlis PRO* 1.171.41.112a (Rigaku OD, 2021), *CrysAlis PRO* 1.171.41.93a (Rigaku OD, 2020), *SHELXT-2014/5* (Sheldrick, 2015), *SHELXL-2016*/6 (Sheldrick, 2015), *SHELXL-2014*/7 (Sheldrick, 2015).
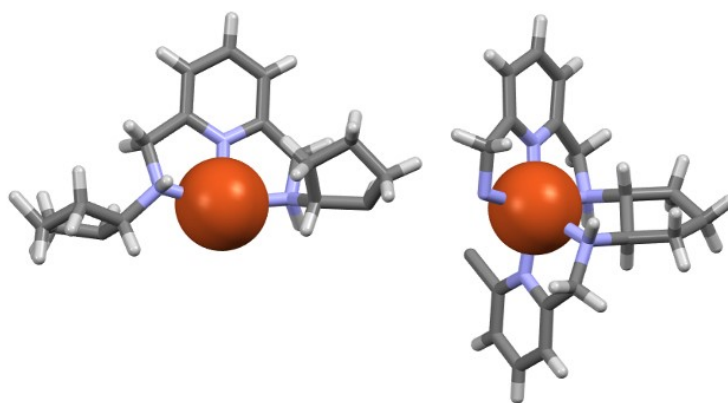
Figure S1. Coordination modes of Cu(II) ion with macrocyclic ligand in Cu(II) complexes. Colour code: Cu, orange; N, blue; C, grey; H, white.
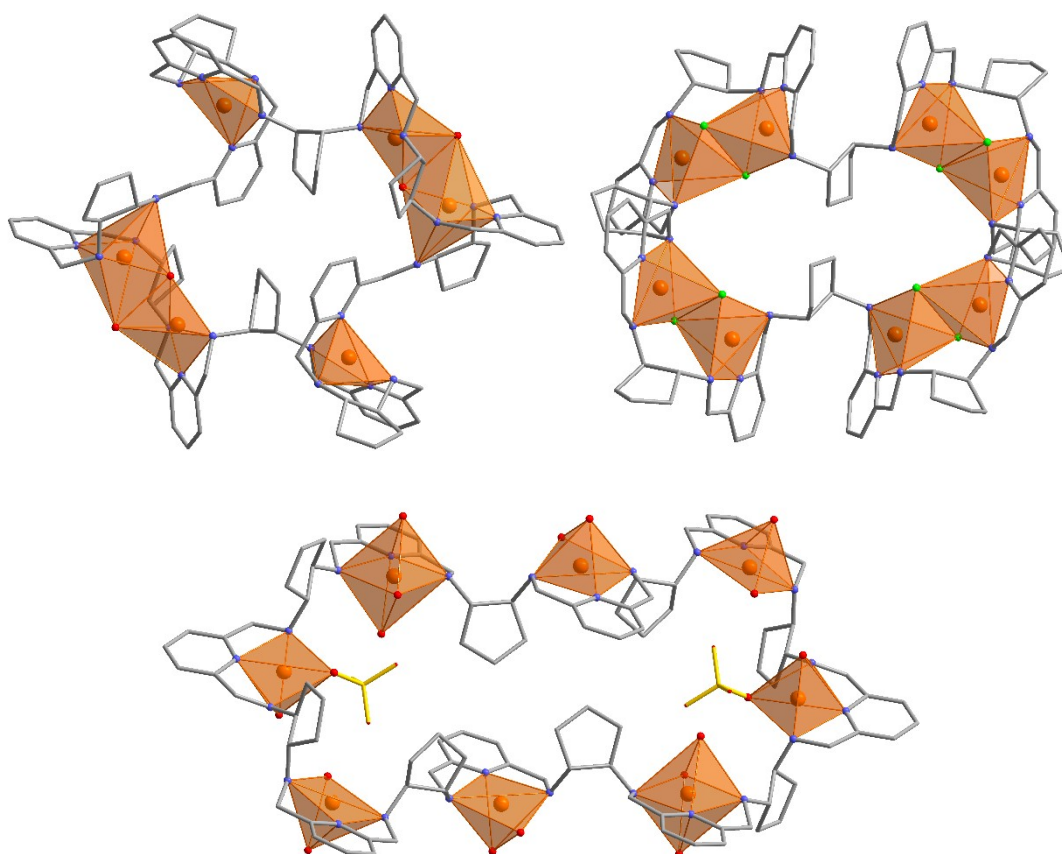

Figure S2. Coordination cations in **1'**, **2'**, and **3'** with the coordination polyhedra of the Cu^{II} ions shown. Hydrogen atoms and disorder of the organic ligand omitted for clarity. Colour code: Cu, orange; N, blue, O, red, S, yellow.
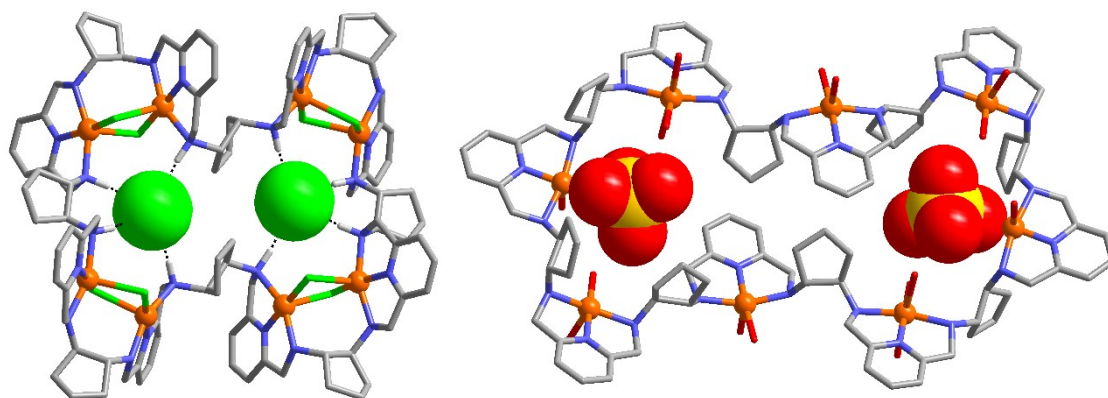
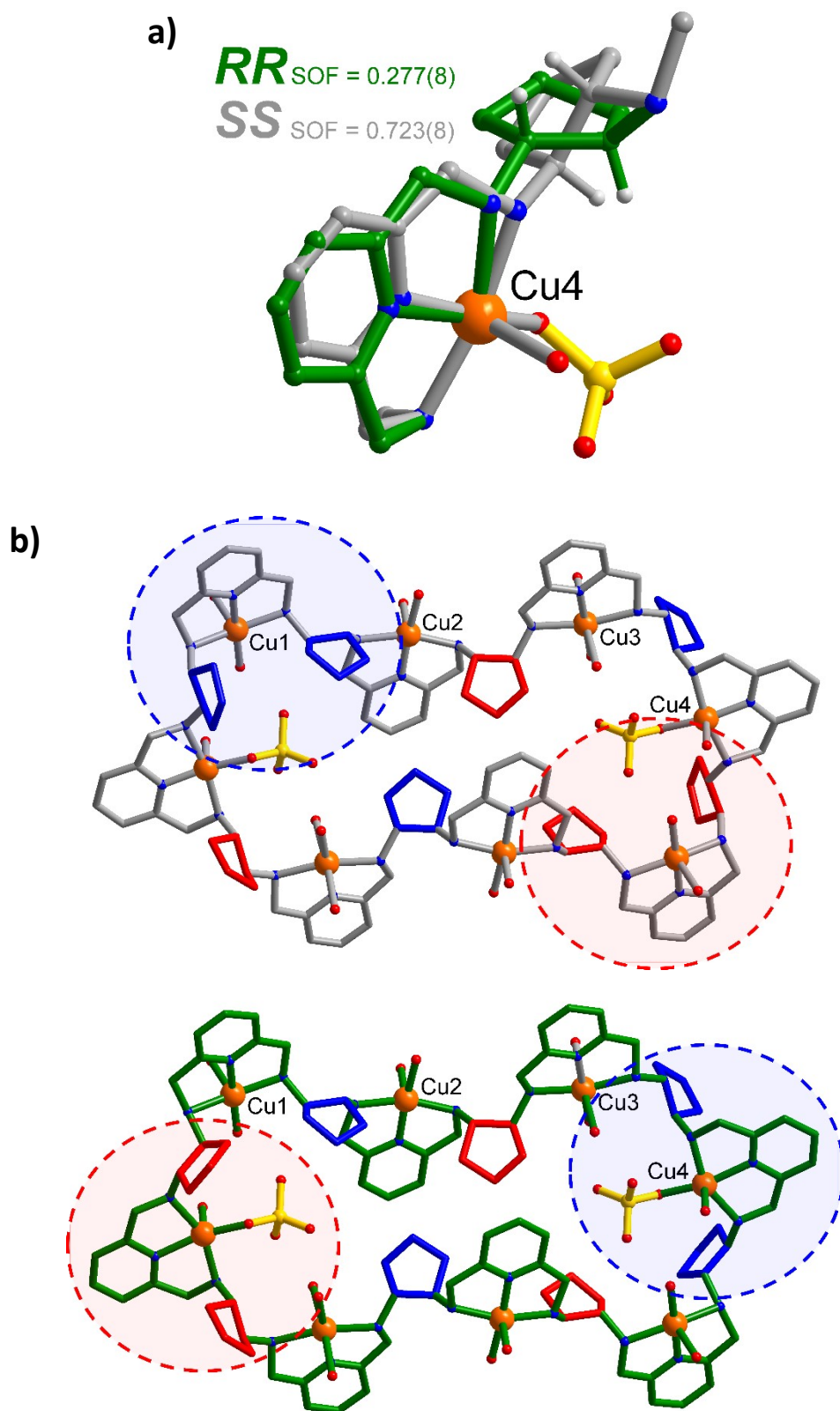**Figure S3**. Occupation of macrocyclic cavities in **2'** and **3'** complexes.

Figure S4. Disordered of the ligand in **3'**. a) Two positions shown with different colours. Hydrogen atoms at asymmetric carbon atoms are shown. b) Two different coordination modes of the same ligand resulting from the ligand disorder model. Colour code for bonds: grey and green – the individual positions of the disordered ligand, blue and red – *RR* and *SS* absolute configuration of the DACP unit, respectively. Colour code for atoms: Cu – orange, S – yellow, O – red, N – blue, C – grey, H – light grey. Blue and red circles indicate homochiral environments of the Cu^{II} cations.
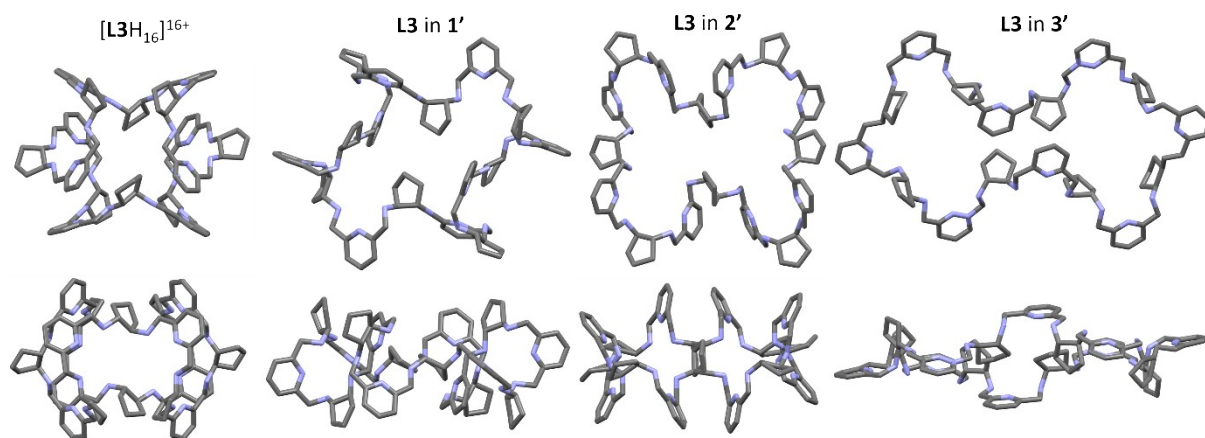
Figure S5. Comparison of the macrocycle **L3** conformations in its protonated form[19] [**LH**$_{16}$]$^{16+}$ and in its multinuclear Cu(II) complexes **1'** , **2'** and **3'**.
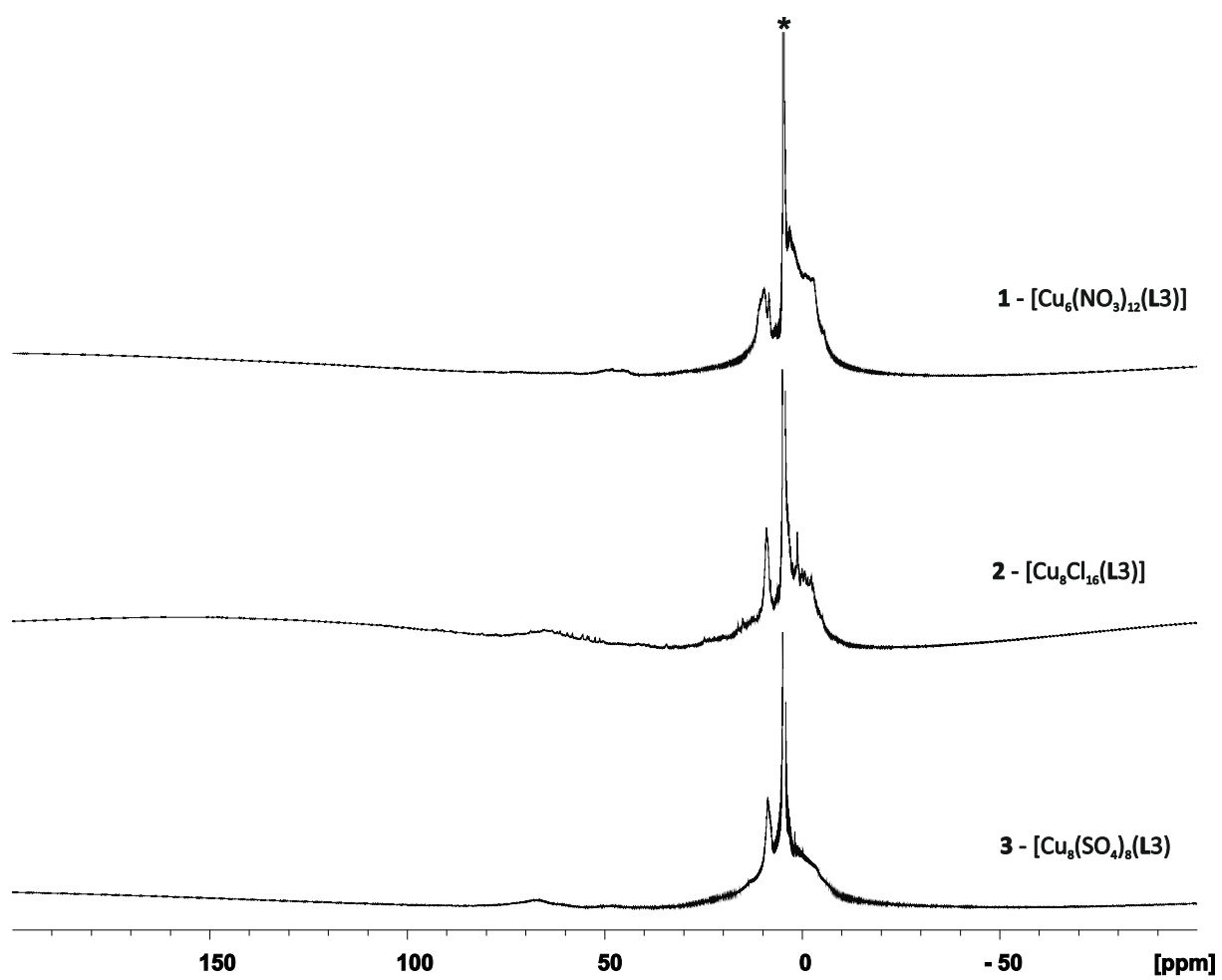
Figure S6. ^{1}H NMR spectra (500 MHz, D_2O) of **1**, **2** and **3** Cu(II) complexes, respectively. Asterisks denotes the residual signal of solvent.
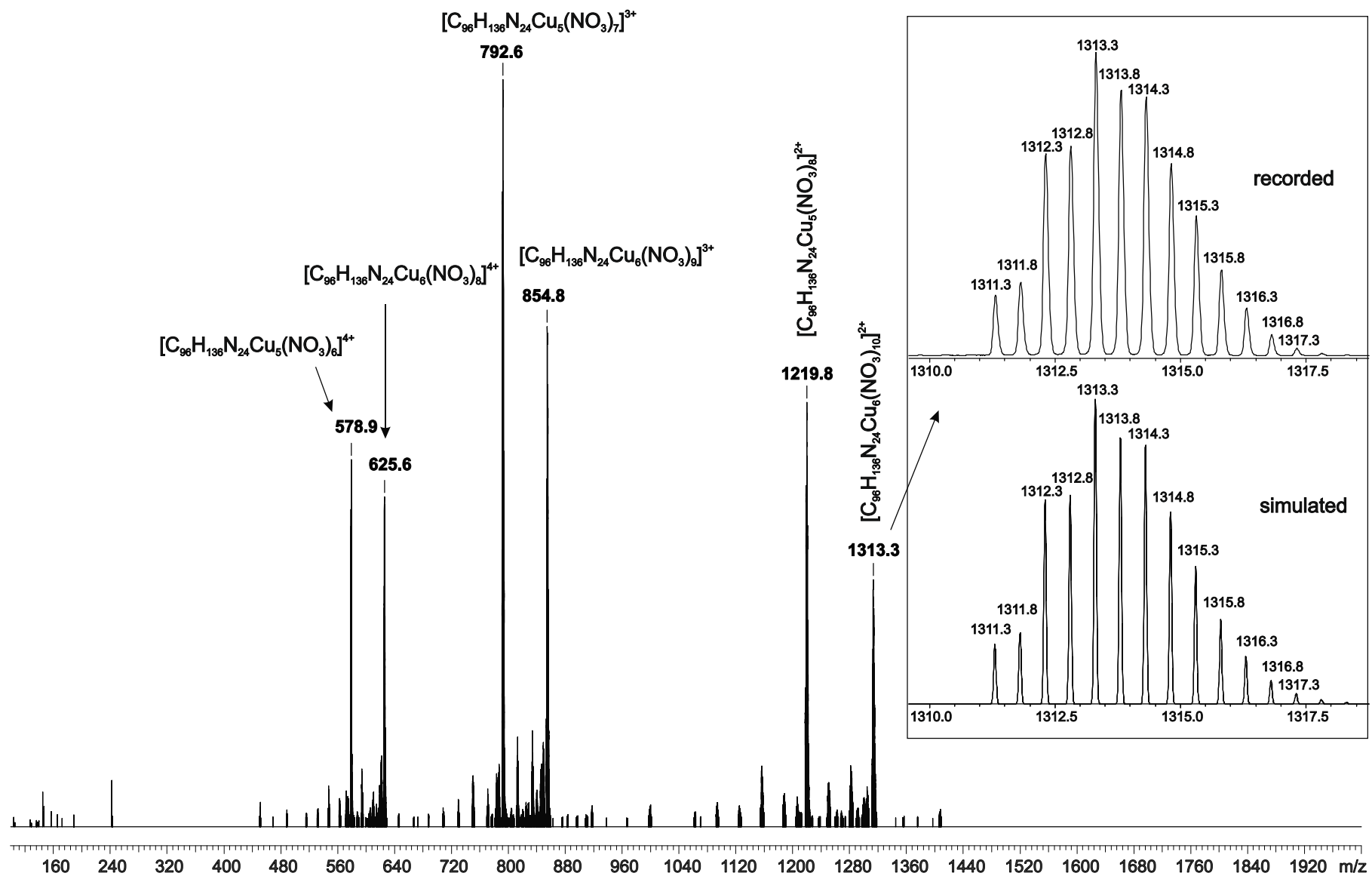
Figure S7.ESI MS spectrum of $[Cu_6(NO_3)_{12}(C_{96}H_{136}N_{24})]\cdot 9H_2O$ complex - **1**. Spectral pattern of the main peak in the frame.
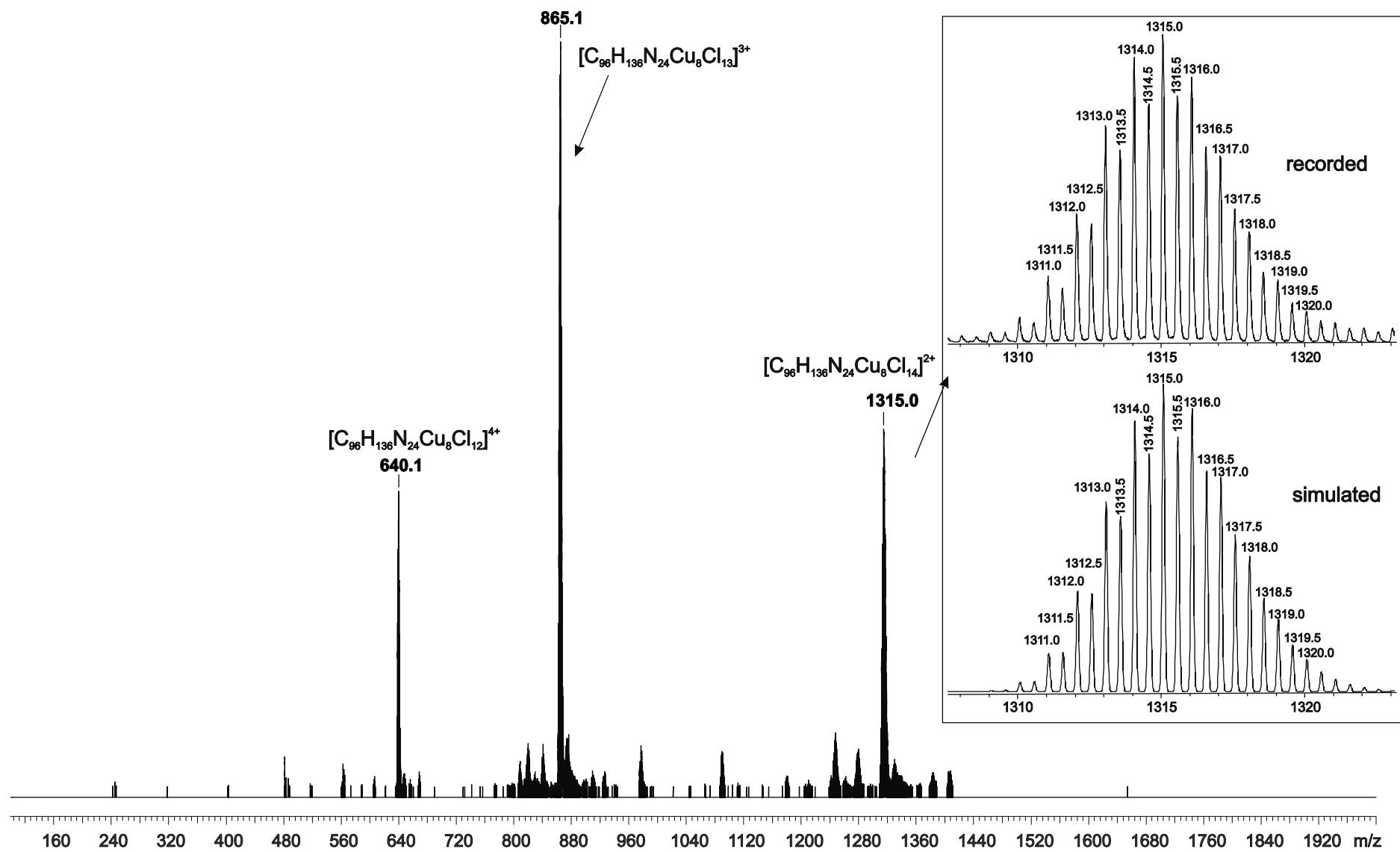
Figure S8. ESI MS spectrum of $[Cu_8Cl_{16}(C_{96}H_{136}N_{24})]\cdot 5H_2O$ complex - **2**. Spectral pattern of the main peak in the frame.
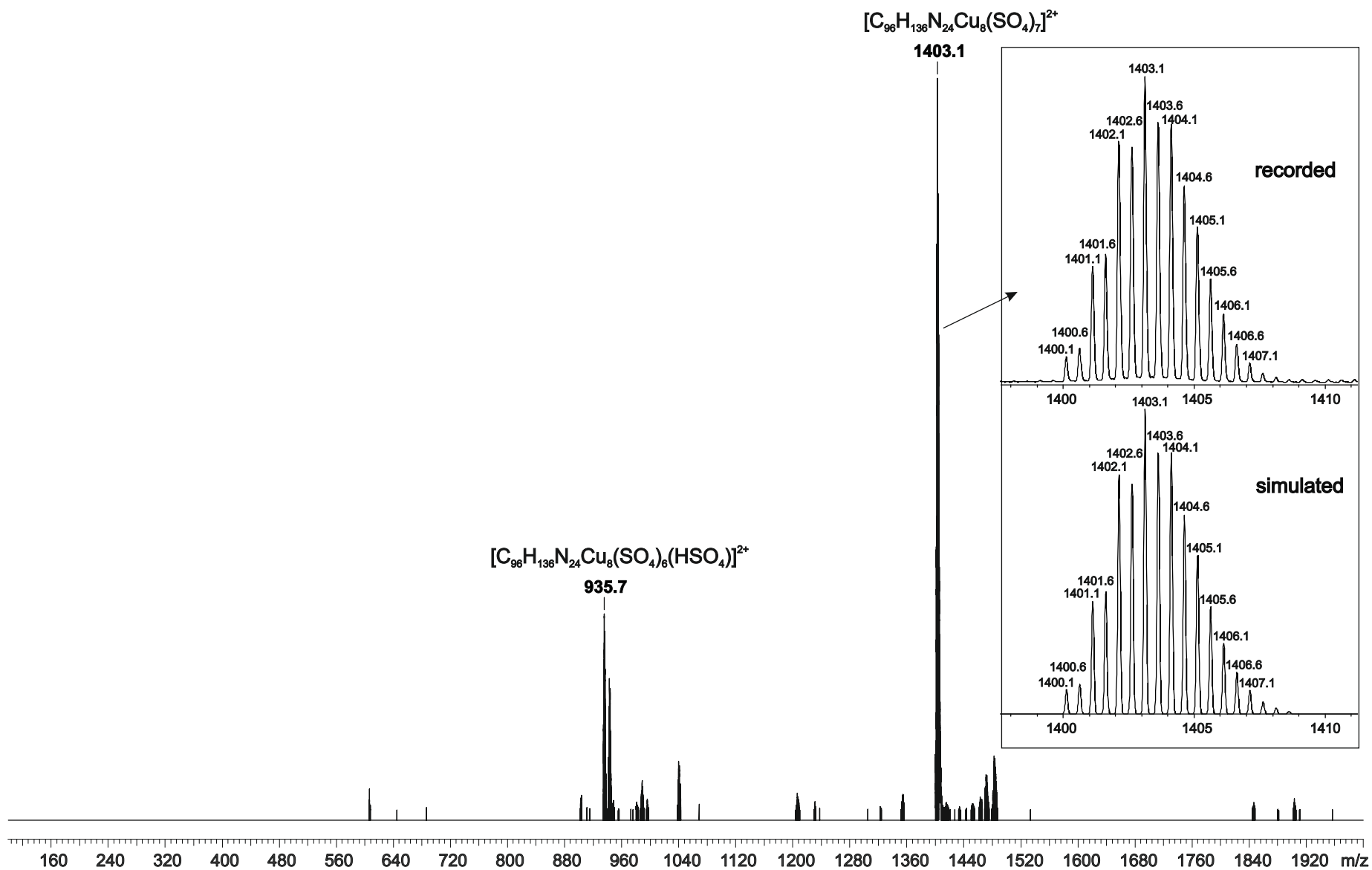
Figure S9. ESI MS spectrum of $[Cu_8(SO_4)_8(C_{96}H_{136}N_{24})]\cdot 37(H_2O)$ complex - **3**. Spectral pattern of the main peak in the frame.

Magnetic properties of Cu(II) complexes

The thermal evolution of χ_m^{-1} obeys the Curie-Weiss law in the whole temperature range. A fit of χ_m^{-1} to the Curie–Weiss law gives a negative and relatively small Weiss temperatures (ϑ) of $-$ 1.92 K (**1**), - 2.45 K (**2**). and - 3.35 K (**3**). The small and negative ϑ values could also confirm the small magnitude of antiferromagnetic exchange in **1-3**.

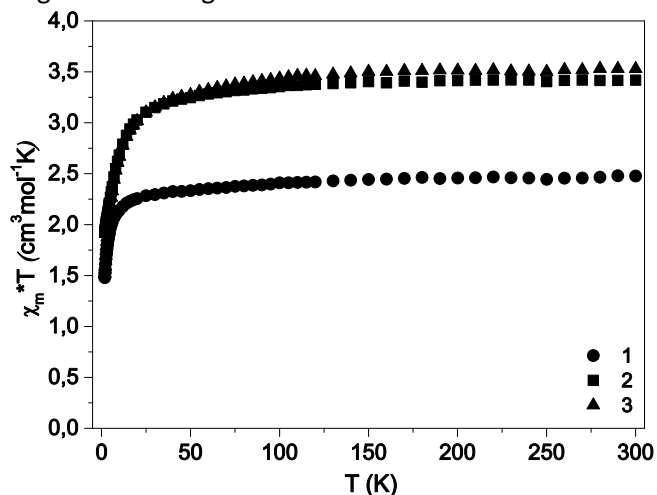**Figure S10.** Temperature dependence of experimental χmT for 1 (●), 2 (■) and 3 (▲) (χm per Cu6 and Cu8 units, respectively).

Magnetization studies verified the nature of the ground state of **1-3** at 2 K in the field range of 0−7 T (**Figure S9**, **ESI†**). The *M* versus *H* curves show a sharp increase in magnetization at a low field limit with a linear response to the magnetic moment upon increasing the magnetic field without saturation. The experimental values are slightly below the values calculated with the Brillouin function for six or eight non-interacting copper(II) ions ($S = ^1/_2$) and confirm our previous assumption.

Such magnetic behaviour may be understood in terms of the nature of the orbitals involved in the exchange interactions, together with the structural characteristics of the bridging network. It is also known that a change in electron density of the magnetic orbital can have a pronounced effect on the sign and magnitude of a magnetic exchange interaction.[48–50] Weak magnetic exchange interactions between copper(II) ions in **3** result from relatively long Cu···Cu distances and lack of bridging anions. The analysis of the crystal structures of **1** and **2** showed the presence of hydroxide and chloride o anions act as bridging ligands, respectively. However, there was no significant effect of the linkers on the exchange interactions. The overlap between the magnetic orbitals of the metal ions through the chloride bridge in **1** and **2** is significantly weak, presumably arising from a more trigonal character of the one copper(II) environment and the electron delocalization on the d_z^2 magnetic orbitals. No efficient path for the exchange interactions in **1-3** was additionally confirmed by EPR spectra.
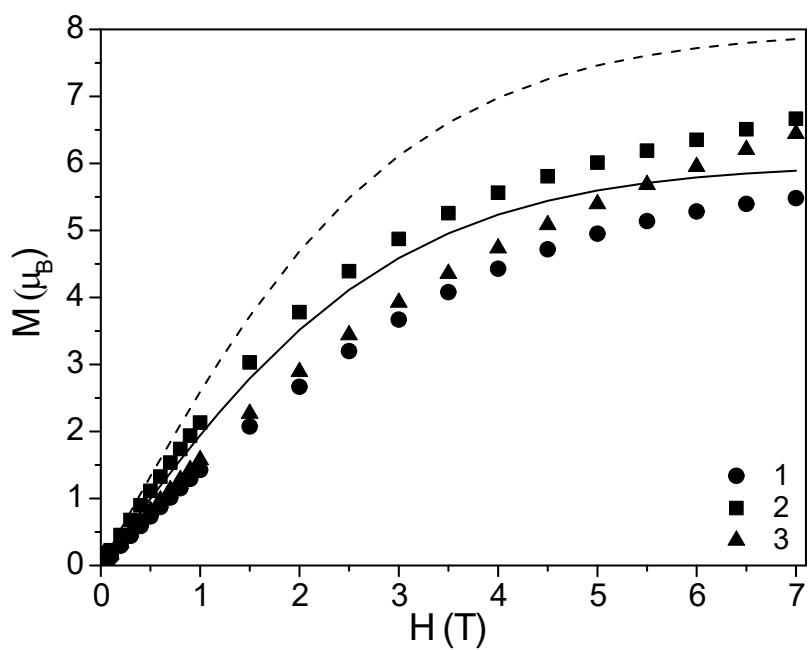
Figure S11. Field dependence of the magnetization for **1** (●), **2** (■) and **3** (▲) (M per Cu_6 and Cu_8 units, respectively) at 2 K. The solid line is the Brillouin function curve for the system of six uncoupled spins with $S = 1/2$; dashed line is the Brillouin function for eight noninteracting $S = 1/2$ systems; $g = 2.0$.

EPR studies on Cu(II) complexes

EPR measurements were conducted using a Bruker Elexsys E500 spectrometer operating at a frequency of approximately 9.7 GHz (X-band). The spectrometer was equipped with an NMR teslameter (ER 036TM) and a frequency counter (HP5342A). All spectra were recorded at 77 K. Powder spectra were recorded for the carefully ground crystalline samples and solution spectra in methanol/ethylene glycol mixture (4:1, v:v) at a concentration of 10 mg/mL. All EPR spectra were simulated using EasySpin 5.2.35.[51]
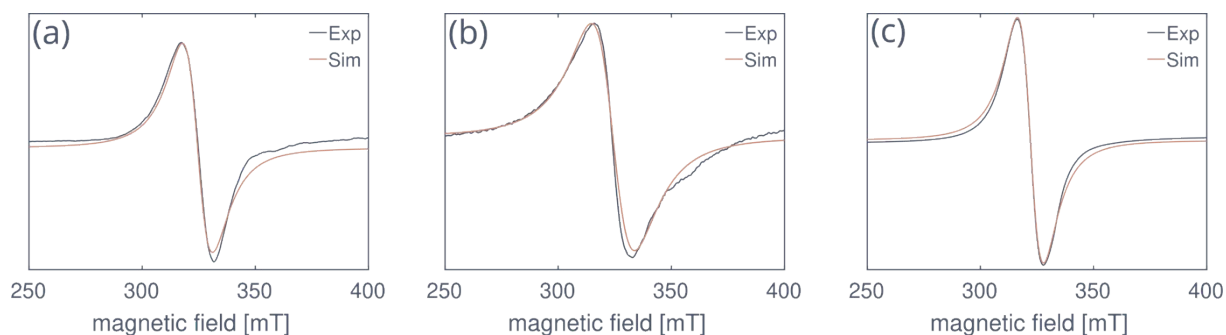

Figure S12. EPR spectra recorded at 77 K for powder samples of **1** (a), **2** (b) and **3** (c). Grey lines indicate experimental spectra, whereas brown lines simulated spectra.

Table S2. Details of EPR simulations shown in **Fig. 4** in the main text.

				Solution				
	Powder	Sim 1		Sim 2				
complex	g	g	weight	g_z	g_x	g_y	A_z [MHz]	weigth
1	2.11	2.10	0.90	2.39	2.08	2.08	400	0.10
2	2.11	2.11	0.83	2.39	2.08	2.08	400	0.17
3	2.13	2.12	0.86	2.39	2.08	2.08	400	0.14

References: See the main text.